Preparation of Macroporous Metal Films from Colloidal Crystals

Peng Jiang, Joel Cizeron, Jane F. Bertone, and Vicki L. Colvin*

Department of Chemistry, Rice University
Houston, Texas 77005
Received April 26, 1999

Template-directed syntheses have been broadly applied to the creation of both meso- and macroporous ceramics[1−4] and polymers.[5] The extension of such methods to metals is of particular interest. Monolithic metals containing large internal surface areas could be used in numerous applications, ranging from electrochemical sensors[6] to catalytic converters.[7] Moreover, recent work on lithographically prepared metallodielectric structures suggests metals with well-ordered porous networks would exhibit interesting photonic properties.[8] The adaptation of template methods to the formation of porous metals has been relatively limited.[9−12] Lyotropic liquid crystalline[12] and anodic alumina[10] have been used as templates to produce mesoporous (voids <50 nm) metal films with parallel and cylindrical pores; however, techniques to make macroporous (voids >50 nm) and high void volume porous films have not yet been reported. In this work we describe a strategy for extending the general methodology of template-directed synthesis to the formation of porous metals. These samples are three-dimensional highly ordered, free-standing macroporous metal films with interconnected spherical voids (200−400 nm). We use as templates single-crystal colloidal multilayers made by a vertical deposition technique.[13]

The uniform deposition of metals into colloidal arrays is challenging for several reasons. Existing examples of metal deposition into lyotropic liquid crystal[12] and anodic alumina[10] templates exploit flat and conductive surfaces to catalyze metal formation. Such surfaces are not available in the interstitial regions of colloidal crystals which are narrow and relatively inaccessible. Also, these templates as made are relatively fragile and easily disrupted by agitation or gas evolution during deposition. To overcome these obstacles, a metal nanocrystal catalyzed electroless deposition technique[14,15] has been developed.

First, colloidal silica is coated with a coupling agent,[16] 3-mercaptopropyltrimethoxysilane (3-MPTMS), which leaves a free thiol functionality at the surface. After vertical deposition of the arrays onto glass substrates,[13] the silica−air templates are immersed in a toluene solution containing gold nanocrystals[17] that affix to the colloidal surfaces at the thiol sites.[16] These nanocrystals have average diameters of only 5 nm and are small enough to penetrate the tiny pores of the template matrix uniformly, covering ∼20% of the available surface. Then, the dried silica−nanocrystal composite is heated in air by a propane

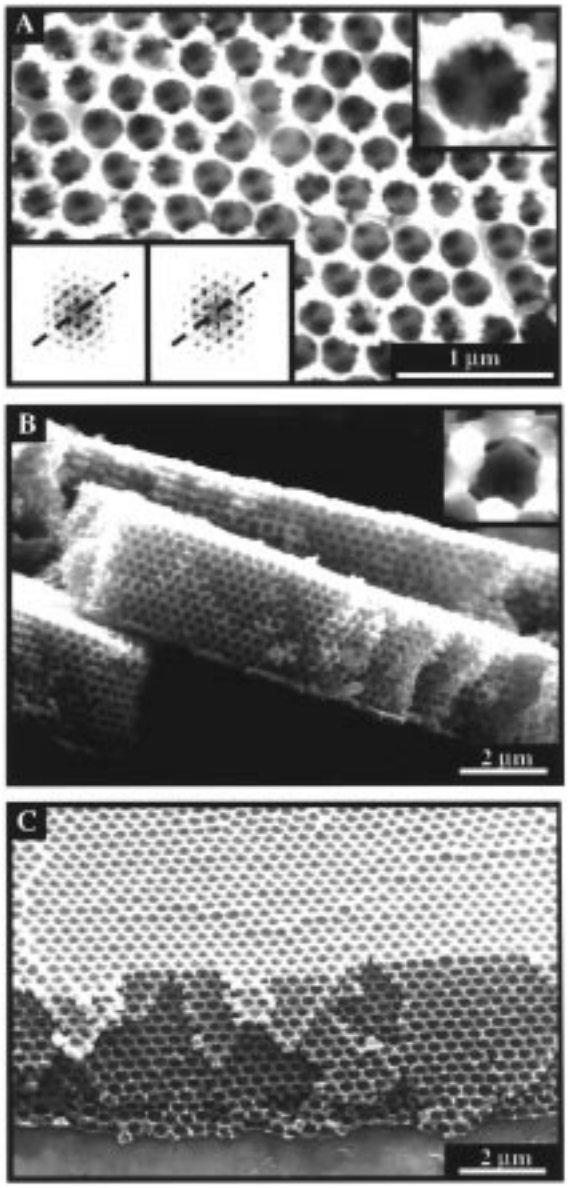

Figure 1. Typical SEM images of three macroporous metal films. (A) Top view of a platinum film with 318 ± 13 nm diameter voids. Bottom left insets show FFTs of two images (15.75 × 11.75 μm area) taken at opposite corners of a 4 × 8 mm region. Upper right inset shows interconnecting pores and rough surface of the same sample. (B) Cross-sectional view of a copper film with 325 ± 15 nm diameter voids revealing porous morphology throughout the film. The inset shows interconnecting pores and smooth surface of the same sample. (C) A nickel film made from a colloidal template (353 ± 17 nm diameter) with 15 colloidal layers. SEM was performed on a Philips XL30 ESEM operating at 30 kV.

(1) (a) Yang, P.; Deng, T.; Zhao, D.; Feng, P.; Pine, D.; Chmelka, B. F.; Whitesides, G. M.; Stucky, G. D. *Science* **1998**, *282*, 2244. (b) Kresge, C. T.; Leonowicz, M. E.; Roth, W. J.; Vartuli, J. C.; Beck, J. S. *Nature* **1992**, *359*, 710.
(2) Velev, O. D.; Jede, T. A.; Lobo, R. F.; Lenhoff, A. M. *Nature* **1997**, *389*, 447.
(3) Holland, B. T.; Blanford, C. F.; Stein, A. *Science* **1998**, *281*, 538.
(4) Wijnhoven, J. E. G. J.; Vos, W. L. *Science* **1998**, *281*, 802.
(5) (a) Johnson, S. A.; Ollivier, P. J.; Mallouk, T. E. *Science* **1999**, *283*, 963. (b) Zakhidov, A. A.; Baughman, R. H.; Iqbal, Z.; Cui, C.; Khayrullin, I.; Dantas, S. O.; Marti, J.; Ralchenko, V. G. *Science* **1998**, *282*, 897. (c) Park, S. H.; Xia, Y. *Adv. Mater.* **1998**, *10*, 1045
(6) Tierney, M. J.; Kim, H. L. *Anal. Chem.* **1993**, *65*, 3435.
(7) Heck, R. M.; Farrauto, R. J. *Catalytic Air Pollution Control, Commercial Technology*; Van Nostrand Reinhold: New York, 1995; pp 71−112.
(8) Sievenpiper, D. F.; Yablonovitch, E.; Winn, J. N.; Fan, S.; Villeneuve, P. R.; Joannopoulos, J. D. *Phys. Rev. Lett.* **1998**, *80*, 2829.
(9) (a) Martin, C. R. *Science* **1994**, *266*, 1961. (b) Nishizawa, M.; Menon, V. P.; Martin, C. R. *Science* **1995**, *268*, 700.
(10) (a) Routkevitch, D.; Chan, J.; Davydov, D.; Avrutsky, I.; Xu, J. M.; Yacaman, M. J.; Moskovits, M. *Mater. Res. Soc. Symp. Proc.* **1997**, *451*, 367. (b) Masuda, H.; Fukuda, K. *Science* **1995**, *268*, 1466.
(11) Shapovalov, V. *MRS Bull.* **1994**, 24.
(12) Attard, G. S.; Bartlett, P. N.; Coleman, N. R. B.; Elliott, J. M.; Owen, J. R.; Wang, J. H. *Science* **1997**, *278*, 838.
(13) Jiang, P.; Bertone, J. F.; Hwang, K. S.; Colvin, V. L. *Chem. Mater.* **1999**, in press.
(14) For a general discussion of electroless deposition, see: Mallory, G. O.; Hajdu, J. B. *Electroless Plating: Fundamentals and Applications*; American Electroplaters and Surface Finishers Society: Orlando, 1990.
(15) Shah, P.; Kevrekidis, Y.; Benziger, J. *Langmuir* **1999**, *15*, 1584.
(16) Westcott, S. L.; Oldenburg, S. J.; Lee, T. R.; Halas, N. J. *Langmuir* **1998**, *14*, 5396.
(17) Brust, M.; Walker, M.; Bethell, D.; Schiffrin, D. J.; Whyman, R. *J. Chem. Soc., Chem. Commun.* **1994**, 801.

10.1021/ja991321h CCC: $18.00
Published on Web 08/13/1999

Table 1. Energy-Dispersive X-ray (EDX) Analysis and Film Properties of the Macroporous Metals[a]

	energy-dispersive X-ray (EDX) anal of the metal films (atom %)				BET surface	nanocrystalline particle size by X-ray diff (nm)	
sample	O	Si	Au	metal	area (m^2/g)	before heating	after heating
Ni	1.6 ± 0.9	0.7 ± 0.4	0.8 ± 0.5	93.7 ± 1.3	26 (11.8)	2 ± 0.5	47 ± 4
Cu	5.8 ± 1.1	1.2 ± 0.7	1.8 ± 0.8	91.3 ± 0.7	12 (9.8)	1.5 ± 0.3	
Ag	2.8 ± 1.2	2.3 ± 1.0	2.5 ± 0.6	92.5 ± 1.4	12 (10)	27 ± 2	
Au	1.7 ± 1.0	1.2 ± 0.3		95.1 ± 1.3		32 ± 3	
Pt	1.6 ± 0.4	0.6 ± 0.2	0.8 ± 0.3	94.9 ± 0.8		21 ± 2	32 ± 3

[a] EDX analysis was carried out on a Philips XL30 ESEM at 30 kV. Typical concentrations of carbon and byproducts of electroless plating of the macroporous films were below 2% (atom %). XRD was performed on a Siemens D5000 diffractometer using Cu Kα radiation and a Rigaku Geigerflex using Mo Kα for the copper film. For the heating studies, metal−silica films were heated at 500 °C under a vacuum for 5 h. The silica was then removed by HF wash. BET experiments were performed on a Coulter SA3100 using nitrogen absorption. Thicker samples were prepared for BET using a filtration method[3] to make the silica colloidal crystal, which was then exposed to gold nanoparticles and annealed at 800 °C for 2 h before templating by methods described above. Values shown in parentheses are surface areas calculated assuming smooth spherical voids.

torch for 5 min, or in a 575 °C oven for 8 h. This heating strengthens the colloidal crystal and removes organics from the gold surfaces. The templates are then immersed in electroless deposition baths, and metal formation in the pores readily occurs.[18] As expected, the metals deposit deep within the template; transmission electron microscopy (TEM) at intermediate times reveals metal curving around the silica spheres as expected for a template process (see Supporting Information). One advantage of using electroless methods is that there exists standard recipes for the deposition of virtually any metal.[14] In this work, we demonstrate the application of this method with nickel, copper, gold, platinum, and silver. After the metal is deposited in the interstitial areas, the silica can be etched away by a 2% HF rinse leaving behind a free-standing porous metal film.

Figure 1 shows scanning electron microscopy (SEM) images of typical macroporous metal films as viewed from both the top and the side. The cavities match the size of the starting silica colloids and retain their close-packed ordering. Higher magnification images of the structures show that each larger cavity in these materials is connected to its twelve neighbors by smaller pores of 60 ± 10 nm diameter (see top insets of Figure 1, A and B). On the basis of their location and number, connecting pores appear to form around the points where the original silica spheres once touched; such a morphology has been observed for other porous materials made using colloidal crystal templates.[4,5] The long-range order of the voids is apparent from Fourier transforms (FFTs) of these images. Figure 1A (bottom insets) shows two FFTs computed from micrographs of a macroporous platinum sample taken more than 8 mm apart. Not only do these FFTs show the spot pattern expected for a perfect hexagonal array, but their orientations are nearly coincident. Images taken at intermediate points also show similar orientation, indicating that the hexagonal arrangement of the voids contains no grain boundaries over length scales as long as millimeters.[13] This long-range order is crucial to the applications of these materials in optics, and indeed these samples exhibit striking iridescence under white light illumination.

An important issue to address is the extent to which the metals infiltrate the template during deposition; cross-sectional images of these materials and measurements of their average surface area provide ample evidence that these samples are uniformly porous up to the maximum thickness studied (10 μm). Figure 1 (parts B and C) shows cross-sectional micrographs of representative macroporous metals; the spherical voids extend throughout both samples with no bubbles or gaps. Figure 1B also shows the structural integrity of the samples. Nickel in particular makes tough and sturdy free-standing films, while gold and silver films often curl and fragment into smaller pieces if not backed with solid metal. Surface area measurements of bulk samples are also consistent with a uniformly porous morphology (Table 1). If metal deposition had not occurred fully throughout the templates, the films would possess larger internal cavities which would lower the measured internal surface areas.[19]

Crystallinity and chemical composition of the metals can be evaluated using energy-dispersive X-ray analysis (EDX) and powder X-ray diffraction (PXRD). EDX of the cross-sections of these films indicates that electrodeposited metals are quite pure (Table 1). Only trace silicon is detected, indicating the complete removal of the template. X-ray diffraction shows reflections characteristic of polycrystalline metallic films (see Supporting Information). Domain sizes in these samples range from 20 to 30 nm for silver, platinum, and gold to 1−3 nm for copper and nickel (Table 1). Given this microstructure, it would be reasonable to expect that measured surface areas would have contributions both from the large air cavities and from surface roughness. Thus, it is not surprising that the measured surface areas are systematically larger than those calculated by a model that neglects surface roughness.

As-prepared samples are not very mechanically or thermally stable, but can be handled if sufficiently thick; vigorous sonication (50 W, 5 min) fractures the films and, in the case of copper, completely destroys its porosity. Moreover, thermal treatment of macroporous nickel results in a reduction of porosity at temperatures of only 500 °C. To strengthen the macroporous metal, the metal−silica composite can be heated prior to silica removal under vacuum. This treatment causes significant grain coarsening in all metals (Table 1), yet has little effect on the long-range order and morphology of the pores. Once sintered, macroporous nickel is able to withstand prolonged sonication and heating under vacuum to 500 °C; macroporous platinum retains its porosity up to 1000 °C in air.

This work demonstrates the generalization of a template methodology to the production of porous metals. Samples possess high internal surface areas which are accessible via an interconnected porous network; this morphology may be of value in applications which rely on the chemical activity of metal surfaces. Moreover, long-range ordering of the porous structure endows the samples with striking optical properties which are the subject of ongoing study.

Acknowledgment. We would like to thank Dean Bertone and Wei Lu for assistance with characterization and Dr. Daniel Mittleman for many useful discussions. This work was supported by the National Science Foundation (CHE-9702520) and the R. A. Welch Foundation (C-1342).

Supporting Information Available: Scheme of the synthesis, TEM of two intermediate stages, and PXRD patterns of macroporous metal films (PDF). This material is available free of charge via the Internet at http://pubs.acs.org.

JA991321H

(18) Electroless plating of copper is performed at room temperature by the technique described by Kim et al. (Kim, E.; Xia, Y.; Whitesides, G. M. *J. Am. Chem. Soc.* **1996**, *118*, 5722). A Technic EN 9148 low phosphorus electroless nickel bath (Technic Inc., RI) is used ($T = 87$ °C) to plate nickel. A commercial silvering bath (HE-300, Peacock Laboratories, Philadelphia, PA) is used to plate silver at room temperature. A commercial gold electroless plating solution (Oromerse SO, Technic Inc.) is used to plate gold ($T = 70$ °C). Electroless plating of platinum is performed at room temperature by the technique described by Rhoda et al. (Rhoda, R. N.; Suffern, N. Y.; Vines, R. F.; Chatham, N. J. U.S. patent 3,486,928, 1969).

(19) Surface areas are calculated by assuming spherical air voids (215 nm diameter) fill 74% of the volume of the metal. No attempt is made to correct for the loss of surface area caused by the interconnections between pores, or for the enhancement of surface area due to surface roughness.